

## Research



Article submitted to journal

**Subject Areas:**

Granular matter

**Keywords:**granular systems, phase separation,  
low-dimensional dynamical systems,  
numerical simulations**Author for correspondence:**

Patricio Cordero

e-mail: [pcordero@dfi.uchile.cl](mailto:pcordero@dfi.uchile.cl)Effect of the vibration profile  
on shallow granular systemsPatricio Cordero<sup>1</sup>, Dino Risso<sup>2</sup> and  
Rodrigo Soto<sup>1</sup><sup>1</sup> Departamento de Física, Facultad de Ciencias  
Físicas y Matemáticas, Universidad de Chile, <sup>2</sup>  
Departamento de Física, Facultad de Ciencias,  
Universidad del Bio-Bio

We describe the collective behavior of a system of many inelastic spherical particles inside a box which is being periodically vibrated. The box is shallow, with large horizontal dimensions, while the height is less than two particle diameters. The vibrations are not symmetric: the time the box is moving up is, in general, different to the time it is moving down. The limit cycles of isolated grains are largely affected by the asymmetry of the vibration mode, increasing the size in phase space of the chaotic regions. When many grains are placed in the box, the phase separation between dense, solid-like regions, coexisting with fluid-like regions takes place at smaller global densities for asymmetric vibration profiles. Besides, the order parameter of the transition takes larger values when asymmetric forcing is used.

## 1. Introduction

Granular systems, characterized by the dissipative collisional dynamics of macroscopic objects still defy our understanding. When energy is injected at a high enough rate to compensate for the dissipated energy dynamical states are generated. Granular media, in many aspects, resemble molecular fluids. However, the energy dissipated at every collision permanently keeps those systems in a non-equilibrium state. The origin of the non-equilibrium states is that energy injected by one mechanism—for example collisions with the walls—is dissipated by a different one, interparticle collisions. A necessary condition for equilibrium would be detailed balance which is not present in our system.

It has been shown that varying the injection mechanism generates non-equilibrium states with different properties. For example, the shear viscosity varies from case to case. Compare the outcomes in Ref. [1], where the Inelastic Hard Sphere model is used in all cases, but the driving mechanism is different. Hence it is interesting to study the different behaviors of the system when different energy injection mechanisms are used.

A particular geometry to study granular systems that has gained interest is the quasi two-dimensional (Q2D) configuration. In this case grains are put in a shallow box: large horizontal dimensions and a rather small vertical one. The box is vertically vibrated and the spherical grains gain energy colliding with the top and bottom plates. This energy is partly transferred to the horizontal directions through collisions.

Using shallow boxes has many advantages. In experiments, it allows the dynamics of the granular layer to be fully visualized by imaging the system, as all particles can be seen and recorded with a camera from the top. This makes it possible to accurately study the system in a microscopic way, as particle's positions and velocities can be measured for most particles at any time. Also the collective behavior can be captured [2–6]. Implied by the energy injection mechanism, the horizontal kinetic energy of the grains can be quite different from the vertical kinetic energy [7,8].

When the height of the box is less than twice the particle's diameter we have a particular and relevant case: no two particles can be on top of one another. Here, gravity does not play a direct role in the horizontal dynamics and the indirect effects can be controlled and reduced by means of increasing the dimensionless acceleration of the box. More importantly, gravity is perpendicular to the eventual directions of phase separation, allowing to discard many known mechanisms. Nevertheless, experiments and simulations have shown that segregation can also take place between grains that differ in size or mass [8,9].

It has been observed that a particular phase separation takes place in shallow boxes: grains form solid-like regions surrounded by fluid-like ones having high contrasts in density, local order and granular temperature [2]. This phase separation is driven by the negative compressibility of the effective two dimensional fluid [3] and, depending on the height of the box, it can be either of first or second order [10,11].

In the present article we study the role that the energy injection plays in the phase separation in Q2D systems. To do so, keeping the material properties and geometry of the system unchanged, we vary the waveform profile of the vibration. That is, we change the pure sinusoidal profile where the upward and downward phases are symmetric, to asymmetric profiles where both phases take different times. Under these conditions we first analyze the dynamics of isolated grains looking for the limit cycles that each one of them develops. For the case of an isolated particle with no top wall see [12–14]. Next we consider dense regimes where the grains interact so that phase separation may take place. It is found that asymmetric vibration profiles increase the size of the chaotic regions in phase space and also facilitate phase separation. Our main tool are event driven molecular dynamics simulations, making use of our own quite efficient strategy [15]. See also [16].

## 2. The Model

### (a) System setup

The grains are inelastic hard spheres with rotational degrees of freedom. These particles are in a vertically vibrated *shallow box*, namely we consider granular systems in a box with a height of the order of two particle diameters and much larger horizontal dimensions. Collisions are characterized by normal and tangential restitution coefficients as well as friction coefficients.

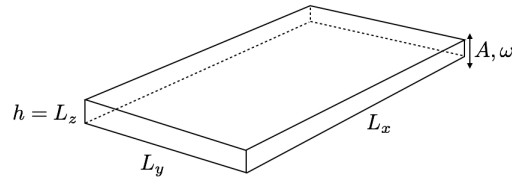


**Figure 1.** Configuration of the quasi two-dimensional granular system. The box is periodic in the horizontal directions, while it is confined by the top and bottom hard walls. The inner height is  $h$ . Grains are placed inside the box, which is vertically vibrated with amplitude  $A$  and angular frequency  $\omega$ .

The diameter  $\sigma$  of the particles, the acceleration of gravity  $g$  and the mass  $m$  of the particles are used to define the dimensionless expressions in this article, except that time is measured in oscillation periods,  $T = 2\pi/\omega$ . The horizontal lengths of the box  $L_x$  and  $L_y$  will be different in different simulations, although in all cases they will be large compared with the confinement height  $h = L_z$ , which is taken to be between  $1.8\sigma$  and  $1.82\sigma$ . Simulations to study the phase separations are done with  $L_z \ll L_y \ll L_x$ , where the system remains homogeneous in the  $y$  direction, allowing us to measure the density contrast between the solid-like cluster and the surrounding liquid-like phase. The vibration is characterized by the amplitude  $A$  and frequency  $\omega$ . Finally, collisions are characterized by the following mechanical parameters: normal and tangential restitution coefficients  $r_n$  and  $r_t$ , while the static and dynamic friction coefficients are  $\mu_s$  and  $\mu_d$ . Their specific values will be given in each case.

### (b) Symmetric profiles: sinusoidal versus parabolic

It may seem natural to consider sinusoidal vibrations, but we have studied systems for which the vibration cycle is characterized by four separate parabolic movements in the sense that the height depends quadratically in time. The acceleration is piecewise constant, with values  $a = \pm 8A\omega^2/\pi^2$ . This parabolic movement is described in detail in the next subsection. It will be interesting to observe that for a given vibration frequency there is a range of amplitudes for which the system behaves almost as if there were sinusoidal vibrations.

### (c) Asymmetric profiles

In our studies energy is injected to the system by means of vertically vibrating the box using asymmetric modes where, again the acceleration is piecewise constant. We define the *asymmetry coefficient*  $\beta$ , ( $0 < \beta < 1$ ), which divides the period in two intervals of size  $\beta T$  and  $(1 - \beta)T$ . In the first interval the box moves down with accelerations  $a = \pm 2A\omega^2/\beta^2\pi^2$ , while in the second one the box moves up with accelerations  $a = \pm 2A\omega^2/(1 - \beta)^2\pi^2$ .

The height  $Z$  of the top (+) and bottom (-) walls of the box are given by

$$Z_{\pm}(t; \beta) = \pm \frac{h}{2} + \alpha(\tau; \beta)A, \quad (2.1)$$

where  $\tau = t \bmod T$  and

$$\alpha(\tau; \beta) = \begin{cases} \frac{1}{\beta^2 T^2} (\beta^2 T^2 - 4\tau^2) & 0 \leq \tau \leq \frac{\beta T}{2} \\ \frac{1}{\beta^2 T^2} (2\tau - \beta T)(2\tau - 3\beta T) & \frac{\beta T}{2} \leq \tau \leq \beta T \\ \frac{1}{(1-\beta)^2 T^2} (2\tau + (1-3\beta)T)(2\tau - (1+\beta)T) & \beta T \leq \tau \leq \frac{(1+\beta)T}{2} \\ \frac{1}{(1-\beta)^2 T^2} (2\tau - (3-\beta)T)((1+\beta)T - 2\tau) & \frac{(1+\beta)T}{2} \leq \tau \leq T \end{cases} \quad (2.2)$$

This function is continuous and has continuous first derivatives. The first derivative of  $\alpha(\tau; \beta)$  vanishes at  $\tau = 0$ ,  $\tau = \beta T$  and at  $\tau = T$ . For  $\beta = \frac{1}{2}$  this quadratic function roughly resembles  $\cos(2\pi\tau/T)$ .

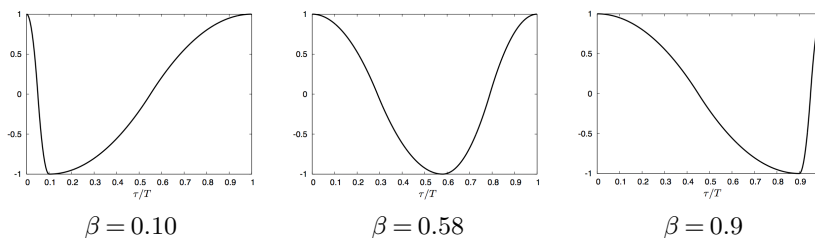


**Figure 2.** The function  $\alpha(\tau; \beta)$  that defines the box-oscillation profile for different values of the asymmetry parameter  $\beta$ . For  $\beta < 1/2$  the downwards interval takes a shorter time than the upward movement (left) and conversely for  $\beta > 1/2$  (right). For  $\beta = 1/2$  the function  $\alpha(\tau; \beta)$  resembles  $\cos(2\pi\tau/T)$ .

The control parameters are the asymmetry parameter  $\beta$ , the amplitude  $A$  and angular frequency  $\omega = 2\pi/T$  of the oscillations. The latter is characterized by the dimensionless acceleration  $\Gamma = A\omega^2/g$  and dimensionless velocity  $\zeta = A\omega/\sqrt{g\sigma}$ .

### 3. A single particle in the vibrating box

In the case of shallow boxes it is important to understand first the movement of a single particle. There are conditions under which the particle ends up in permanent contact with the base of the box. But if  $A\omega^2/g$  is larger than unity such situation cannot occur. Next, it may happen that the energy injected to the particle by the basis is not enough for the particle to reach the upper wall in the long term evolution. We consider conditions under which neither of these last two cases can take place.

If the single particle is left bouncing for a sufficiently large time, its angular and horizontal translation velocities vanish so that the movement of the particle becomes strictly one dimensional and the friction coefficients as well as the tangential restitution coefficient become irrelevant. There is a wide range of amplitudes and frequencies for which the particle reaches this quite simple limit cycle characterized by two velocities: the velocities with which the particle bounces off the two horizontal walls.

Increasing the vibration frequency or the amplitude the limit cycle of the single particle reaches a threshold above which the limit cycle suffers a bifurcation. Now the grain bounces twice at the top and bottom walls before repeating its movement. Hence the new limit cycle takes twice the time associated to the limit cycle just before the bifurcation. There is a chain of bifurcations of this type until the bouncing of the single particle becomes chaotic. Some cases of the resulting limit cycles are presented in Fig. 3. All this can be appreciated in Figure 4 where it is seen that other modes appear as the amplitude grows, that is, the particle has more than one bouncing mode for a

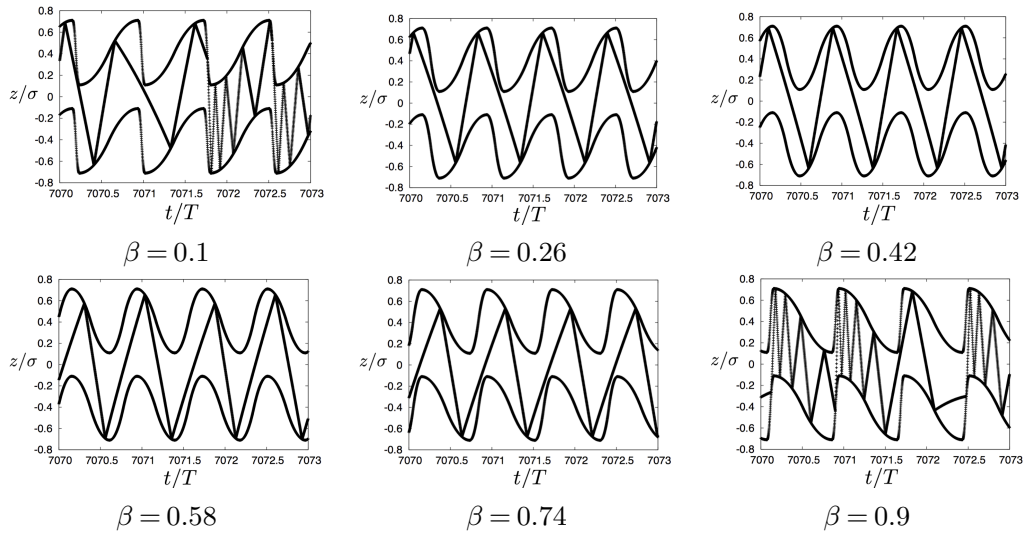


**Figure 3.** A single particle in the shallow box subject to vibrations having the same  $\Gamma$  and  $\zeta$  but different values of  $\beta$  may have quite different stationary bouncing modes. In this example we chose  $\Gamma = 18.56$  and  $\zeta = 2.32$ .

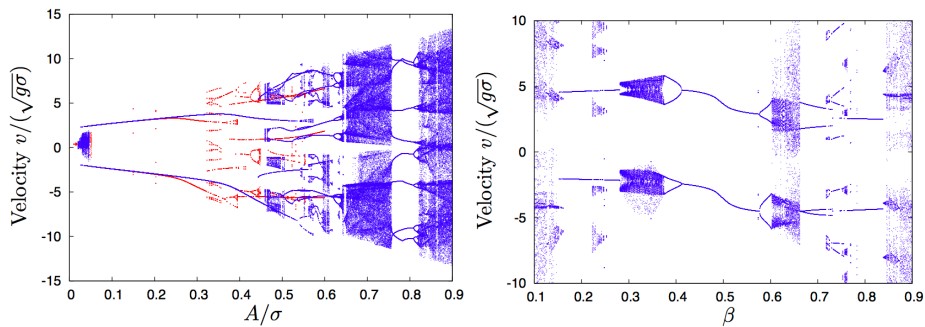
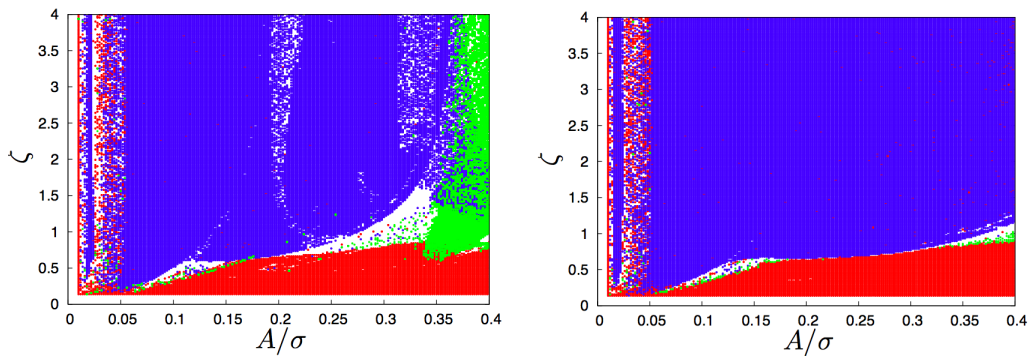


**Figure 4.** Bouncing velocities after colliding with the top and bottom walls of the shallow box once the particle has reached a steady state. Left: Varying the vibration amplitude  $A$  in the case of the sinusoidal (red) and bi-parabolic (blue) symmetric profiles ( $\beta = 1/2$ ). Right: Varying the asymmetry parameter  $\beta$  with fixed vibrating amplitude  $A/\sigma = 0.3$ . The asymmetry on the obtained velocities around  $\beta = 1/2$  is due to the presence of gravity. In both figures,  $\omega = 8\sqrt{g/\sigma}$ ,  $r_n = 0.8$ , and  $h = 1.82\sigma$ . In the right figure  $\Gamma = 19.2$  and  $\zeta = 2.4$ .

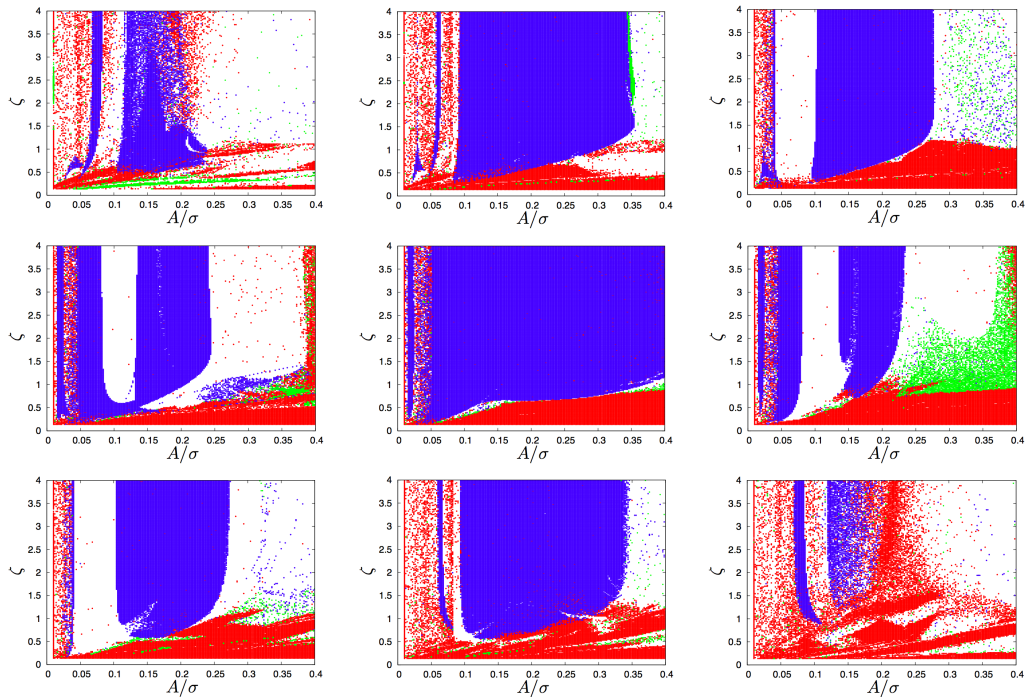
given value of the amplitude. Figure 4 includes in red the bouncing velocities when the vibration is sinusoidal with the same frequency and amplitude as our parabolic vibration. To our surprise, when  $\beta = 0.5$  the bouncing velocities are almost exactly the same till about  $A/\sigma = 0.2$ .

Figure 5 presents a qualitative picture of the possible outcomes. Different colors are used to represent the single period, double period, and chaotic motion cases. The comparison shows how similar is the behavior with sinusoidal and parabolic profiles, except that for large amplitudes the parabolic profiles are more regular. In both cases, a band of chaotic motion is present for small amplitudes.

Using the same analysis, we consider the asymmetric profile, varying the parameter  $\beta$  in the case where in the symmetric profile the limit cycle consists on a single bounce on the top and bottom walls. Figure 4 shows that close to the symmetric case ( $\beta \approx 0.5$ ) the limit cycle is perturbed, keeping its qualitative behavior but changing the values of the bouncing velocities. Further away



**Figure 5.** Map in the  $A$ - $\zeta$  plane of the qualitative characterization of the limit cycles for the sinusoidal profile (left) and for the symmetric  $\beta = 1/2$  parabolic profile (right). The possible outcomes are: bouncing only with the bottom wall with period  $T$  (red), bouncing with the top and bottom walls with period  $T$  (blue), bouncing with the bottom and top walls with double period  $2T$  (green), and more complex states (white). In both cases  $h = 1.8\sigma$  and  $r_n = 0.8$ .



**Figure 6.** Map in the  $A$ - $\zeta$  plane of the qualitative characterization of the limit cycles for different values of  $\beta$  using the same color coding as in Fig. 5. From left to right, top:  $\beta = 0.1, 0.2, 0.3$ , middle:  $\beta = 0.4, 0.5, 0.6$ , bottom:  $\beta = 0.7, 0.8, 0.9$ . In all cases  $h = 1.8\sigma$  and  $r_n = 0.8$ .

from the symmetric condition, period doubling and chaos appears. The qualitative plots in Figure 6 confirm this result. The most regular motion is obtain in the vicinity of  $\beta = 0.5$ . For intermediate values of  $\beta$  figure 6 shows that the effect of gravity is obvious in the case of smaller values of  $\zeta$  while for  $\zeta$  large (small  $g$ ) the structure of the figure is weekly dependent of  $\zeta$ .

## 4. Phase separation

In the case of systems composed by a single species of granular matter there are conditions under which the system separates into high and low density zones [3]. The results of the previous section illustrate a central point: the form of the vibration—determined by the parameter  $\beta$ —has an important effect in the way the system behaves. This is illustrated in Figure 7 which shows a characteristic state of a vibrated granular system in a narrow 3D box: depending on the value of  $\beta$  the system may or may not present phase separation. Indeed, with all other parameters fixed to a case where the symmetric case would yield to a state with no phase separation, forcing with asymmetric profiles induces phase separation.

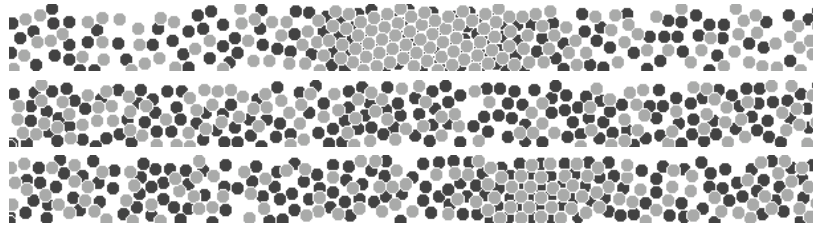


**Figure 7.** Top view of a shallow system in a rather narrow box ( $L_y \ll L_x$ ) in a typical state for a system with common values for all their parameters except for the value of  $\beta$ . Particles are all the same, but they are represented by black circles if their height is below half the height of the box, otherwise they are represented by gray circles. From top down  $\beta = 0.1$ ,  $\beta = 0.5$  and  $\beta = 0.75$ . The first and third cases have notoriously stable phase separated states, showing large density contrasts. In all cases  $N = 410$ ,  $L_x = 90.01\sigma$ ,  $L_y = 4.65\sigma$ ,  $h = 1.8\sigma$ ,  $r_n = r_t = 0.91$ ,  $\mu_d = 0.10$ ,  $\mu_s = 0.17$ ,  $\omega = 10\sqrt{g/\sigma}$ , and  $A = 0.29\sigma$  implying  $\zeta = 2.9$  and  $\Gamma = 29.0$ .

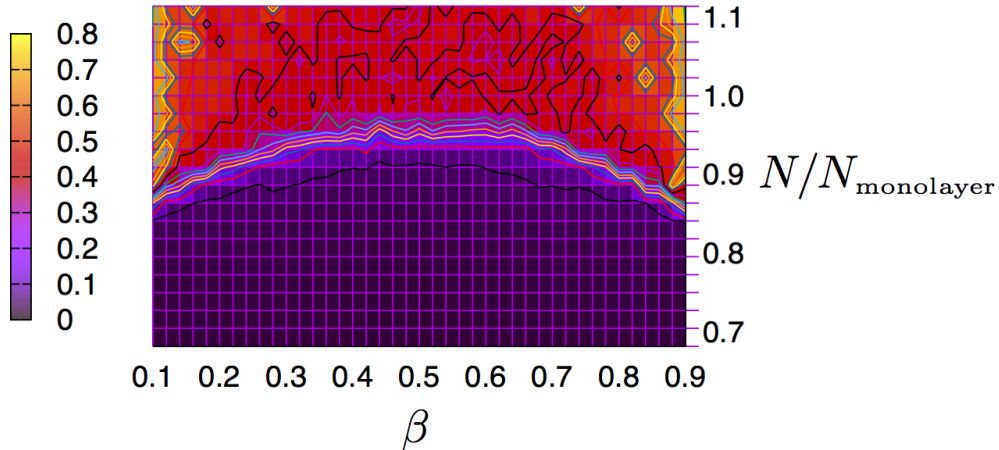


**Figure 8.** Density contrast  $c$  in the  $\beta - N/N_{\text{monolayer}}$  plane for a system with  $L_z = 1.8\sigma$  and  $L_x \times L_y = 90\sigma \times 4.65\sigma$  and vibration parameters  $\tilde{\omega} = \omega/\sqrt{g/\sigma} = 3$  and  $A = 0.29\sigma$ ;  $\zeta = 0.87$ ,  $\Gamma = 2.61$ . The inelasticity and friction grain-grain and grain-wall coefficients are  $r_n = r_t = 0.91$  and  $\mu_d = 0.10$ ,  $\mu_s = 0.17$ .

For a quantitative analysis, we define the *contrast* observable  $c$ , which is the ratio between the smaller and larger observed area densities:  $c = (n_{\text{max}} - n_{\text{min}})/(n_{\text{max}} + n_{\text{min}})$ . In the case of

the system shown in Fig. 7, which are strictly 3D, the density is evaluated considering many transversal strips and calculating the area density in each strip, defined using the projection of the particles in each 2D strip.

Figure 8 shows that, in agreement with the snapshots in Fig. 7, the density contrast is larger when  $\beta$  is away from the symmetric case  $\beta = 0.5$ . A transition line can be identified where there is steep increase in  $c$ . This transition line indicates that away from the symmetric case, a smaller number of particles is needed to produce the phase separation. This is clearly presented in the left panel of Fig. 9, where the contrast is shown as a function of the number of particles for three values of  $\beta$ . A clear transition is observed, with a critical number of particles that is larger for  $\beta = 1/2$ .

Figure 9-right presents the contrast  $c$  as a function of  $\beta$  for a fixed number of particles and different values of  $\omega$ . The collapse between the majority of the curves shows that the mayor impact in the phase separation is the shape of the vibration rather than the energy injection rate.

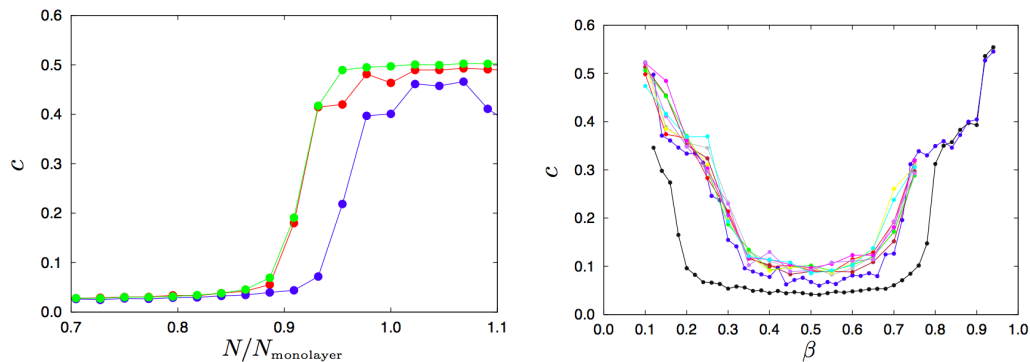


**Figure 9.** Left: density contrast against  $N/N_{\text{monolayer}}$  for  $\beta = 0.22$  (red),  $\beta = 0.5$  (blue) and  $\beta = 0.78$  (green). The amplitude is fixed to  $A = 0.29\sigma$  while the dimensionless frequency takes the value  $\tilde{\omega} = \omega/\sqrt{g/\sigma} = 3$ . Right: density contrast against  $\beta$  for a system with  $N = 410$  grains ( $N/N_{\text{monolayer}} = 0.93$ ). The amplitude is fixed to  $A = 0.29\sigma$  while the dimensionless frequency takes the values  $\tilde{\omega} = 2$  (black),  $\tilde{\omega} = 3$  (blue),  $\tilde{\omega} = 5$  (grey),  $\tilde{\omega} = 10$  (red),  $\tilde{\omega} = 15$  (brown),  $\tilde{\omega} = 20$  (green),  $\tilde{\omega} = 25$  (yellow),  $\tilde{\omega} = 30$  (magenta),  $\tilde{\omega} = 35$  (purple) and  $\tilde{\omega} = 40$  (cyan). In all cases  $L_z = 1.8\sigma$ ,  $L_x \times L_y = 90\sigma \times 4.65\sigma$  and the inelasticity and friction grain-grain and grain-wall coefficients are  $r_n = r_t = 0.91$  and  $\mu_d = 0.10$ ,  $\mu_s = 0.17$ .

## 5. Conclusions

In this article we have studied the role of changing the energy injection profile of the box in vibrofluidized shallow granular media, where the box moves vertically in a periodic way. With this aim we modify the oscillation profile. Originally, the profile was symmetric with piecewise constant accelerations, mimicking a sinusoidal oscillation. This profile was changed to an asymmetric one, still with piecewise constant accelerations, where the downward and upward phases take different fractions of the oscillation period:  $\beta$  and  $1 - \beta$ , respectively.

Single isolated grains reach states where the motion is purely vertical. These states can be periodic in the form of limit cycles with the same period as the box or with a period that is an integer multiple of the box period. Also chaotic or irregular motion is possible. The effect of moving toward asymmetric forcing is to increase the region in parameter space where chaotic motion is observed. Conversely, it is more probable to find regular motion with the same period as the box for the symmetric forcing.

The asymmetric forcing also has an effect on the phase separation between dense and dilute regions when many particles are placed in the box. The phase separation takes place for smaller

number of particles when the forcing is asymmetric. The previous result suggests that other ways of increasing the asymmetry could also be efficient in producing phase separation. As an extreme case, we consider a sawtooth profile at high frequency and small amplitude, such that particles always meet the walls at the same position and approaching the particles with a fixed velocity. Figure 10 shows that indeed phase separation takes place and high contrast states can be attained.

It remains as an open question if there is a relation between the accessibility to chaotic behavior for single particles far from the symmetric profile and the enhanced phase separation in the collective dynamics with many particles.

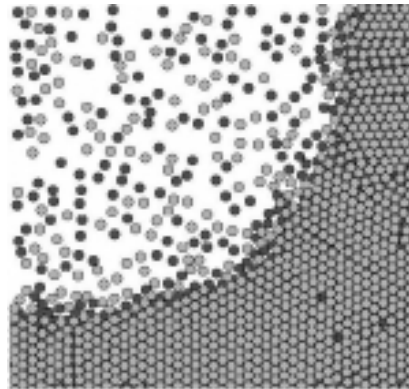


**Figure 10.** Top view of a shallow system in a box of square basis. This is a typical state once phase separation has taken place. The black/grey coloring is as in Fig. 7. The limit of infinitely rapid vibration is taken ( $A \rightarrow 0$ ,  $\omega \rightarrow \infty$ , while  $A\omega = V_0 = \text{constant}$ ) for a sawtooth profile with no gravity. This state was obtained using  $N = 1732$ ,  $L_x = L_y = 40\sigma$ ,  $L_z = 1.9\sigma$ ,  $r_n = r_t = 0.7$  (grain-grain),  $r_n = r_t = 0.999$  (wall-grain), and  $\mu_s = \mu_d = 0.1$ .

In Ref. [3] it was shown that the origin of the phase separation is a negative compressibility region in the effective equation of state of the pressure as a function of density  $p = p(n)$ . This equation of state emerges as a consequence of the temperature being enslaved to the density under high vertical confinement, with  $T(n)$  a monotonically decreasing function. Then, equations of state  $p = p(n, T)$  derived from kinetic theory, with positive compressibility can turn into effective equations of state with negative compressibility and van der Waals loops [17]. An attempt to understand why is it that for  $\beta$  far from 0.5 a phase separation takes place for lower densities it would be necessary to study in the stationary regime the enslaving  $T(n)$ , which will depend on  $\beta$ . This analysis needs the study of the limit cycles coupled with the three-dimensional collisions that transfer energy from the vertical to the horizontal degrees of freedom. This analysis, beyond the scope of this article, is postponed for a further study

The result of the present article as well as others confirm that the properties of non-equilibrium systems depend not only on the internal dynamics but also on the energy injection mechanism. Consistent with this it should be said that there is no guarantee that the conclusions raised here could be valid for other forcing mechanisms.

## 6. Authors contributions

P. Cordero and D. Risso carried out the simulations. All authors participated in the design of the simulations, analysis the results and writing of the manuscript.

**Funding statement.** This research was supported by Fondecyt Grants Nos. 1120775 and 1140778.

## References

1. J.J. Brey, J.W. Dufty, C.S. Kim, and A. Santos, Phys. Rev. E **58**, 4638 (1998). A. Santos, V. Garzó, and J.W. Dufty, Phys. Rev. E **69**, 061303 (2004). P. Cordero, D. Risso, and R. Soto, Physica A **356**, 54 (2005). R. Soto, D. Risso, and R. Brito, Phys. Rev. E **90**, 062204 (2014).
2. J.S. Olafsen, J.S. Urbach, Phys. Rev. Letters **81** 4369, (1998); A. Prevost, P. Melby, D.A. Egolf, and J.S. Urbach, Phys. Rev. E, **70** 050301(R) (2004); P. Melby *et al.*, J. Phys. Cond. Mat. **17**, S2689-S2704 (2005).
3. M.G. Clerc, P. Cordero, J. Dunstan, K. Huff, N. Mujica, D. Risso and G. Varas, Nature Physics **4** 249 (2008).
4. T. Schnautz, R. Brito, C.A. Kruelle, and I. Rehberg, Phys. Rev. Lett. **95**, 028001 (2005).
5. F.F. Chung, S.S. Liaw, and C.Y. Ju, Gran. Matter **11**, 79 (2009).
6. F. Pacheco-Vazquez, Gabriel A. Caballero-Robledo, and J. C. Ruiz-Suarez, Phys. Rev. Lett. **102**, 170601 (2009).
7. P. Melby *et al.*, J. Phys. Condens. Matter **17**, S2689 (2005).
8. N. Rivas, P. Cordero, D. Risso, and R. Soto, New J. Phys. **13**, 055018 (2011).
9. N. Rivas, S. Ponce, B. Gallet, D. Risso, R. Soto, P. Cordero, and N. Mujica, Phys. Rev. Lett. **106**, 088001 (2011).
10. G. Castillo, N. Mujica, and R. Soto, Phys. Rev. Lett. **109**, 095701 (2012).
11. G. Castillo, N. Mujica, and R. Soto Phys. Rev. E **91**, 012141 (2015).
12. A. Mehta and J.M. Luck, Phys. Rev. Letters **65**, 393 (1990); Phys. Rev. E **48**, 3988 (1993)
13. K. Szymanski and Y. Labaye, Phys. Rev. E **59**, 2863 (1999).
14. J.J. Barroso, M.V. Carneiro and E.E.N. Macau, Phys. Rev. E **79**, 026206 (2009)
15. M. Marin, D. Risso and P. Cordero, Journal of Computational Physics **109** 306 (1993), P. Cordero, D. Risso and M. Marin, Chaos, Fractals and Solitons **6** 95 (1995), M. Marin and P. Cordero, SCS 28th Annual Simulation Symposium (ASS 1995), Phoenix, Arizona, April 1995, pages 288-295, Editors: G. Chiola, A. Ferscha, E. Kortright (IEEE-CS Press), M. Marin and P. Cordero, Comp. Phys. Comm. **92**, 214 (1995), M. Marin and P. Cordero, 8th Joint EPS-APS International Conference on Physics Computing, Krakow, Poland, Sept. 1996, pages 315-318, Editors: P. Borchers, M. Bubak (World Scientific, 1996), P. Cordero and M. Marin, Fourth Granada Lectures in Computational Physics, P.L. Garrido and J. Marro, eds, Springer-Verlag, 1997.
16. S. González, D. Risso and R. Soto, Eur.Phys. J. Special Topics **179**, 33 (2009).
17. C. Cartes, M.G. Clerc and R. Soto, Phys. Rev. E **70**, 031302 (2004).